Table S1. Dates, locations, and sub-surface depth of the sampling stations in the Chukchi Sea

Station No.	Sampling date	Latitude (°N)	Longitude (°W)	SSL depth (m)	Bottom depth (m)	The deepest depth measured by the ADCP (m)
9	2020/10/8	70.50	165.50	11	44	31
10	2020/10/10	74.55	161.88	33	1688	271
11	2020/10/11	74.98	158.13	15	841	255
12	2020/10/12	75.18	160.01	15	1985	319
13	2020/10/13	73.29	160.01	32	1212	375
15	2020/10/14	72.79	158.02	15	773	391
17	2020/10/15	71.32	158.44	22	115	87
20	2020/10/15	71.97	153.99	15	740	399
22	2020/10/17	75.01	164.96	26	552	439
23	2020/10/18	75.00	167.24	16	262	207
24	2020/10/18	75.00	169.64	34	236	191
25	2020/10/18	75.00	175.00	27	266	223
26	2020/10/19	75.00	172.02	27	383	311
27	2020/10/19	74.60	170.21	25	208	167
29	2020/10/19	73.50	168.81	18	116	87
31	2020/10/20	72.00	168.83	12	50	31
33	2020/10/20	70.00	168.81	15	39	23
34	2020/10/20	69.03	168.83	16	52	39
35*	2020/10/21	68.01	168.83	26	58	39

*Mooring station

Table S2. Final matrices of pigment /chl a ratio by a chemotaxonomic tool "*phytoclass*"

	Pigment:chl *a* ratio											
	Peri	**butFuco**	**Fuco**	**HexFuco**	**Neo**	**Prasino**	**Viola**	**Allo**	**Lut**	**Zea**	**Chlb**	**Chla**
Diatoms	0	0	0.81	0	0	0	0	0	0	0	0	1
Chrysophytes	0	0.74	0.21	0.05	0	0	0	0	0	0	0	1
Dinoflagellates	1.05	0	0	0	0	0	0	0	0	0	0	1
Prymnesiophytes	0	0	0	0.76	0	0	0	0	0	0	0	1
Chlorophytes	0	0	0	0	0.13	0	0.28	0	0.51	0.05	0.35	1
Prasinophytes	0	0	0	0	0.09	0.19	0.09	0	0	0	0.75	1
Cryptophytes	0	0	0	0	0	0	0	0.23	0	0	0	1
Cyanobacteria	0	0	0	0	0	0	0	0	0	1.05	0	1

Abbreviations: Peri: peridinin, butFuco: 19'-Butanoyloxyfucoxanthin, Fuco: fucoxanthin, HexFuco: 19'-Hexanoyloxyfucoxanthin, Neo: neoxanthin, Prasino: prasinoxanthin, Viola: violaxanthin, Allo: alloxanthin, Lut: lutein, Zea: zeaxanthin, Chlb: chlorophyll *b*, Chla: chlorophyll *a*

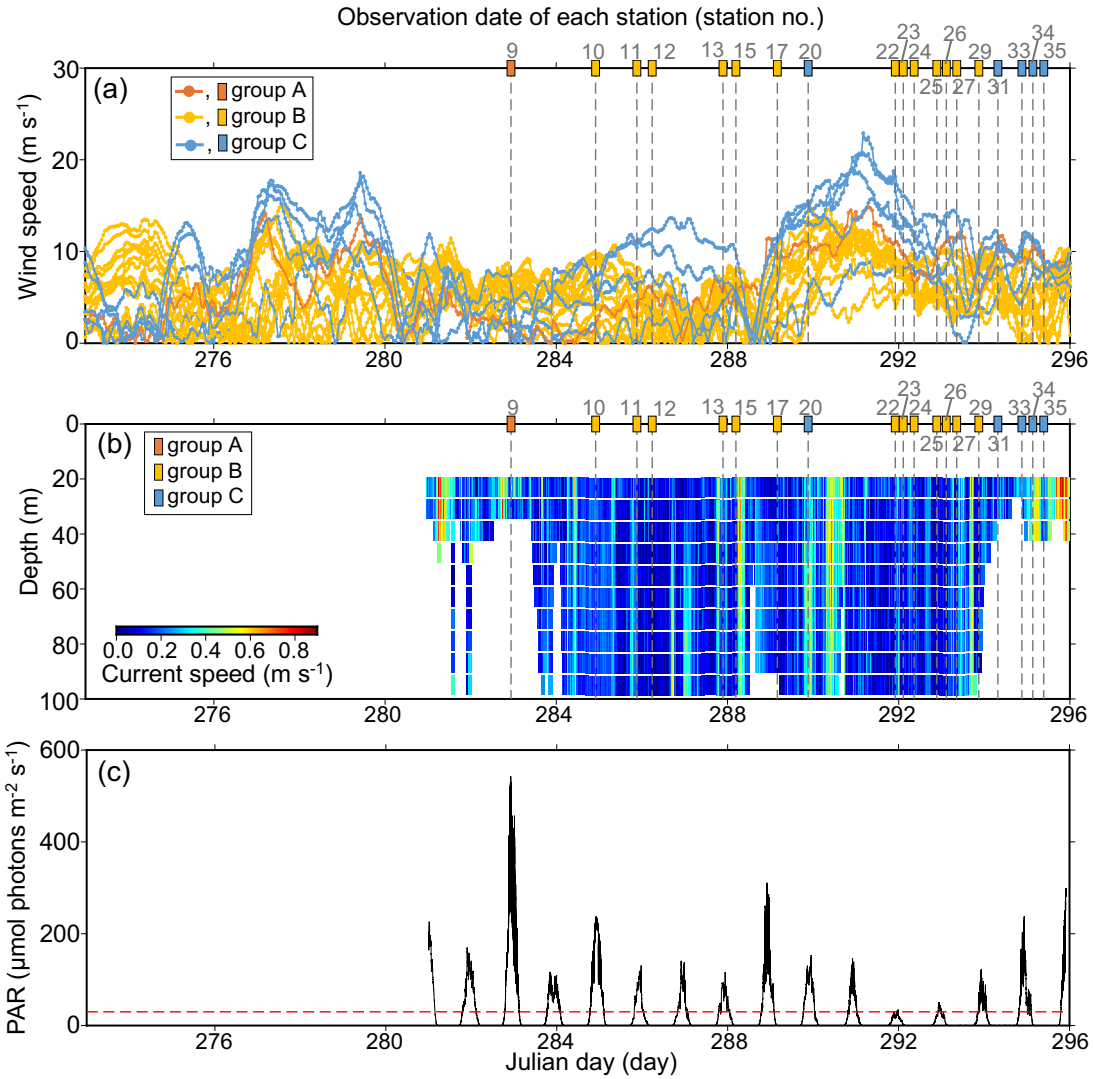

Fig. S1. (a) Wind speeds computed from the ERA5 hourly u- and v-wind components (Hersbach et al.2023). Square plots and numbers indicate the observation date and station numbers during the cruise. (b) Underway data of current speed in the Arctic (north of 66.33°) during the cruise. Square plots and numbers indicate the observation date and station numbers during the cruise. (c) Photosynthetically active radiation (PAR) measured by a shipboard sensor in the Arctic (north of 66.33°) during the cruise. The red dashed line indicates the light intensity; Fukai et al. (2022) demonstrated that the photosynthetic processes of diatoms in sediments reactivate quickly (i.e., when exposed to 30 µmol photons m^{-2} s^{-1}).

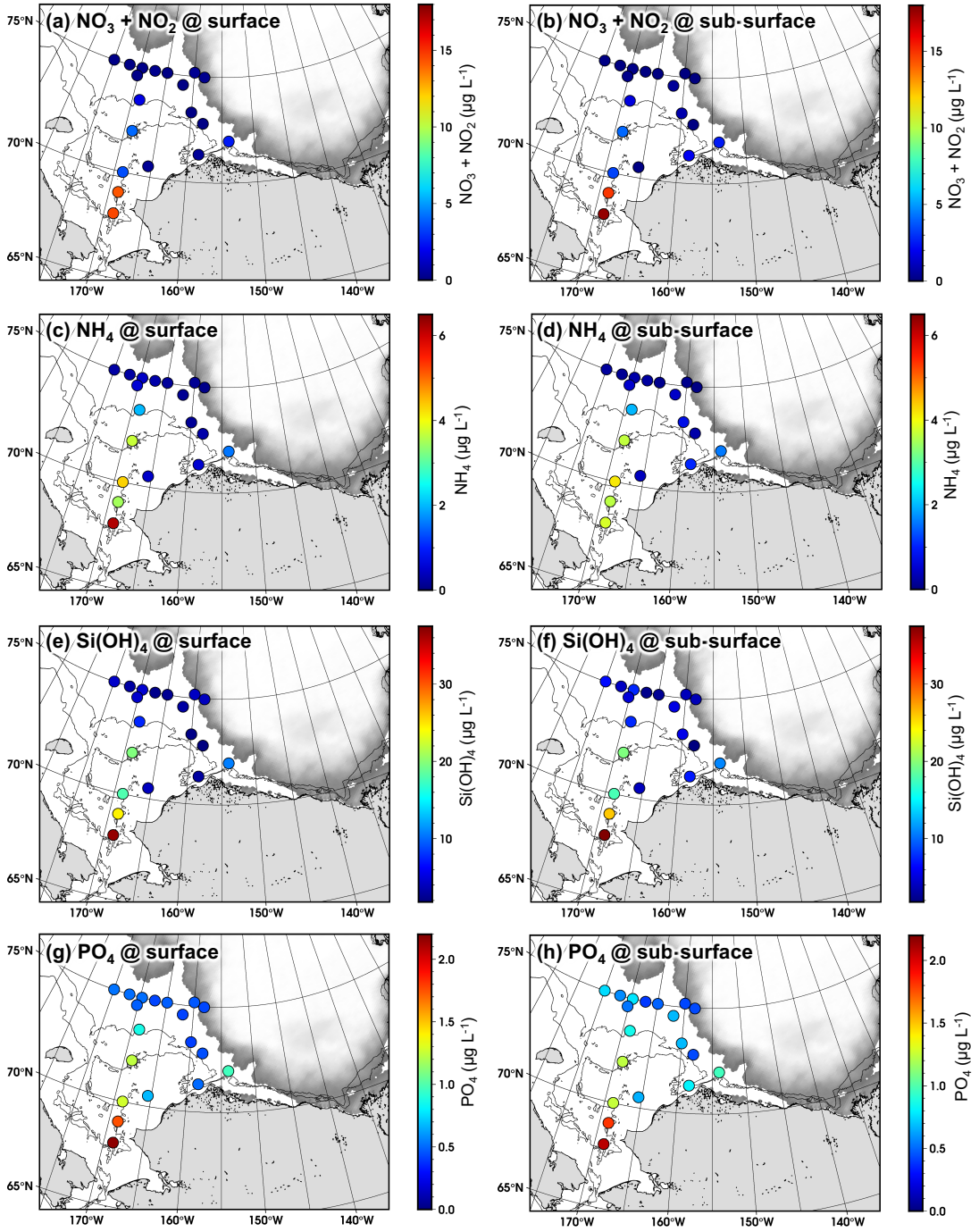

Fig. S2. Spatial distribution of nutrients at the sampling layers.

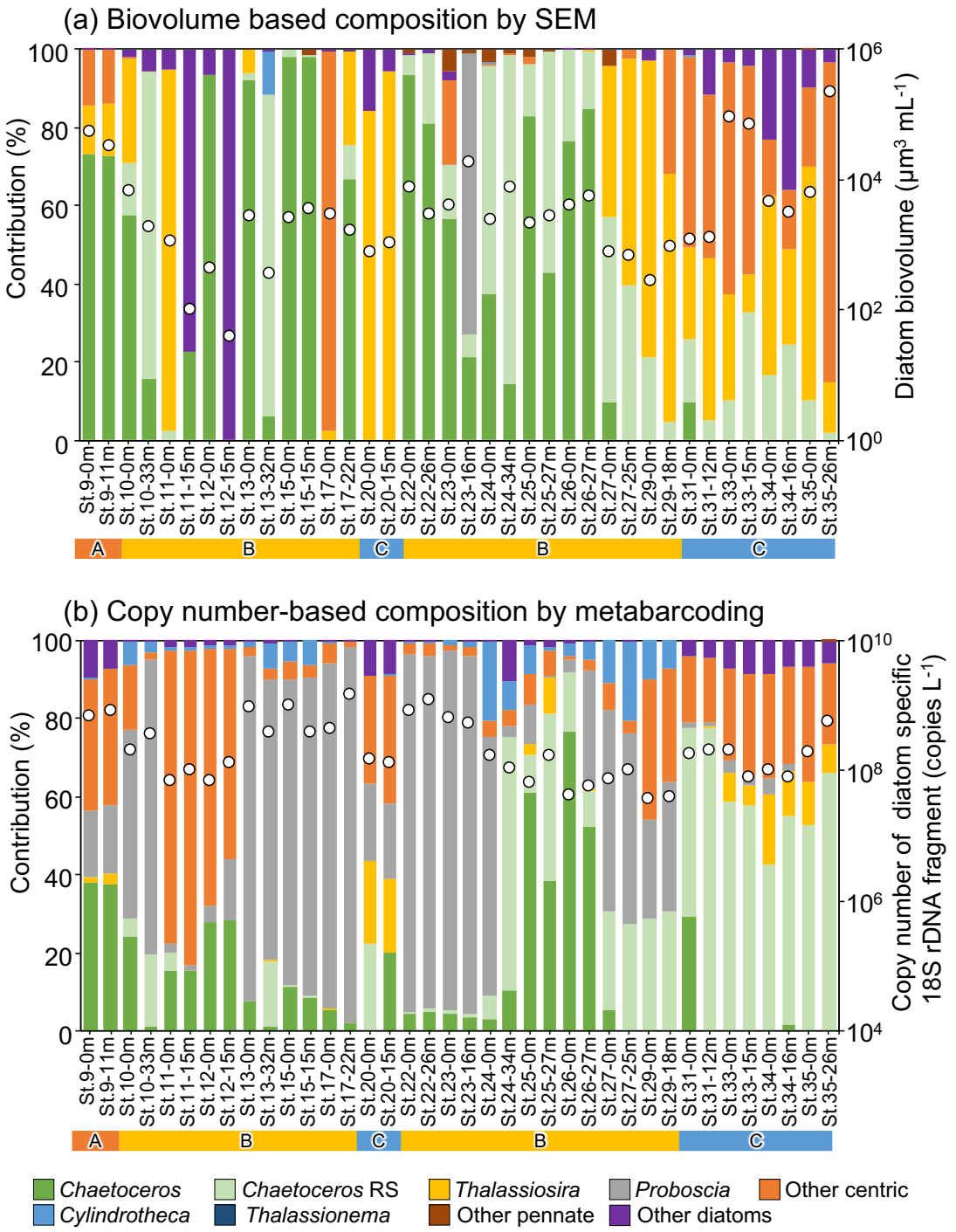

Fig. S3. Diatom composition based on (a) diatom biovolume estimated by SEM and (b) absolute abundance of ASVs. White circles indicate the average diatom biovolume (a) and copy number of diatom-specific 18S rRNA gene fragments (b). The alphabetical bar below the sample name indicates diatom community groups classified by cluster analysis.

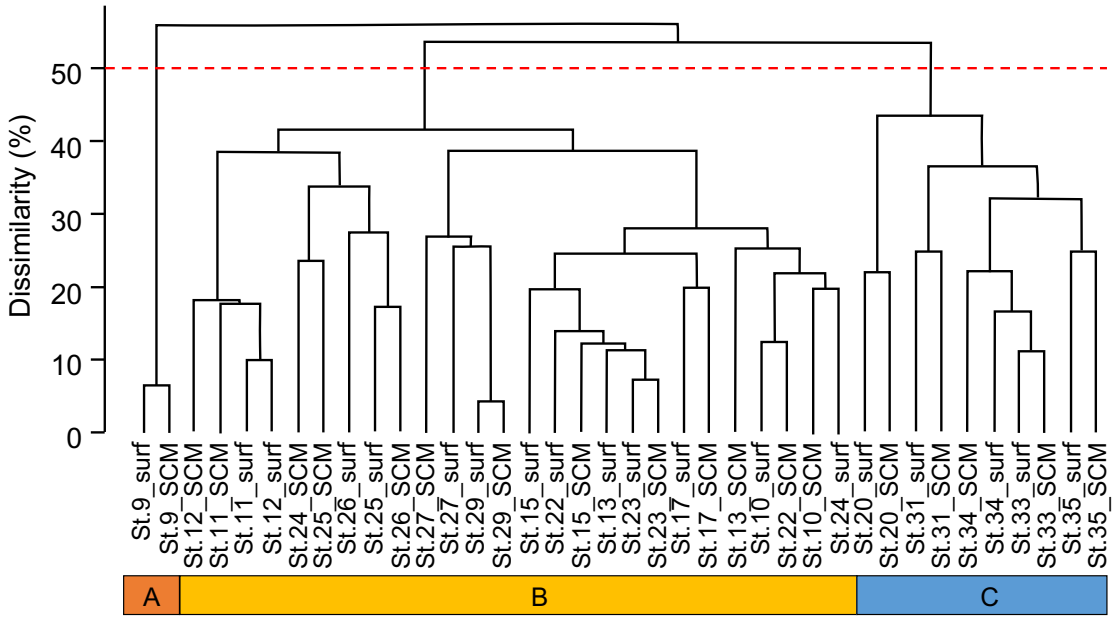

Fig. S4. Dendrogram of cluster analysis. Dissimilarities between samples were examined using the Bray–Curtis index based on the differences in the ASV composition.

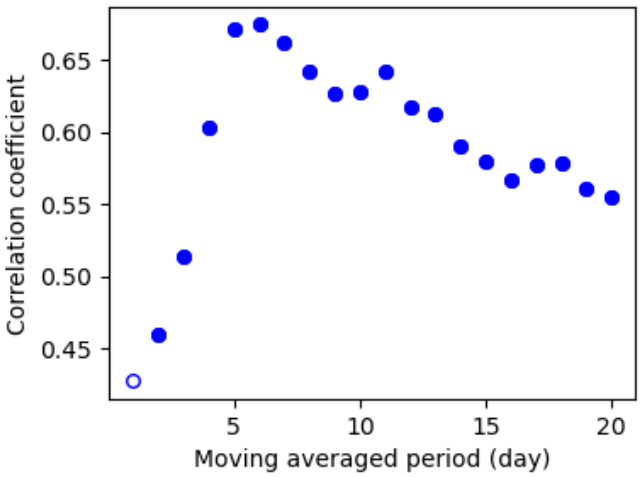

Fig. S5. The relationships between the moving averaged period (day) of wind and the correlation of the wind speed and the current speed at the deepest layer. Filled dots indicate the correlation was significant (p <0.05).

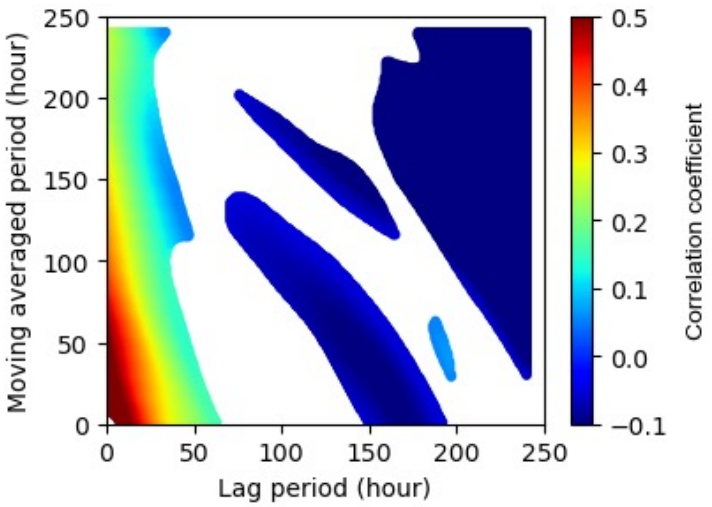

Fig. S6. The relationships of the lag period (hour) between the wind and the current near the bottom, the moving-averaged period (hour) of the wind speed, and the correlation coefficient between the wind speed and the current speed near the bottom (moving average value for 24 hours). The data from September and October were used for the calculation. The correlation coefficient are the average of 2016, 2017, 2018, and 2019. The filled region indicates the correlation was significant in all years ($p < 0.05$).

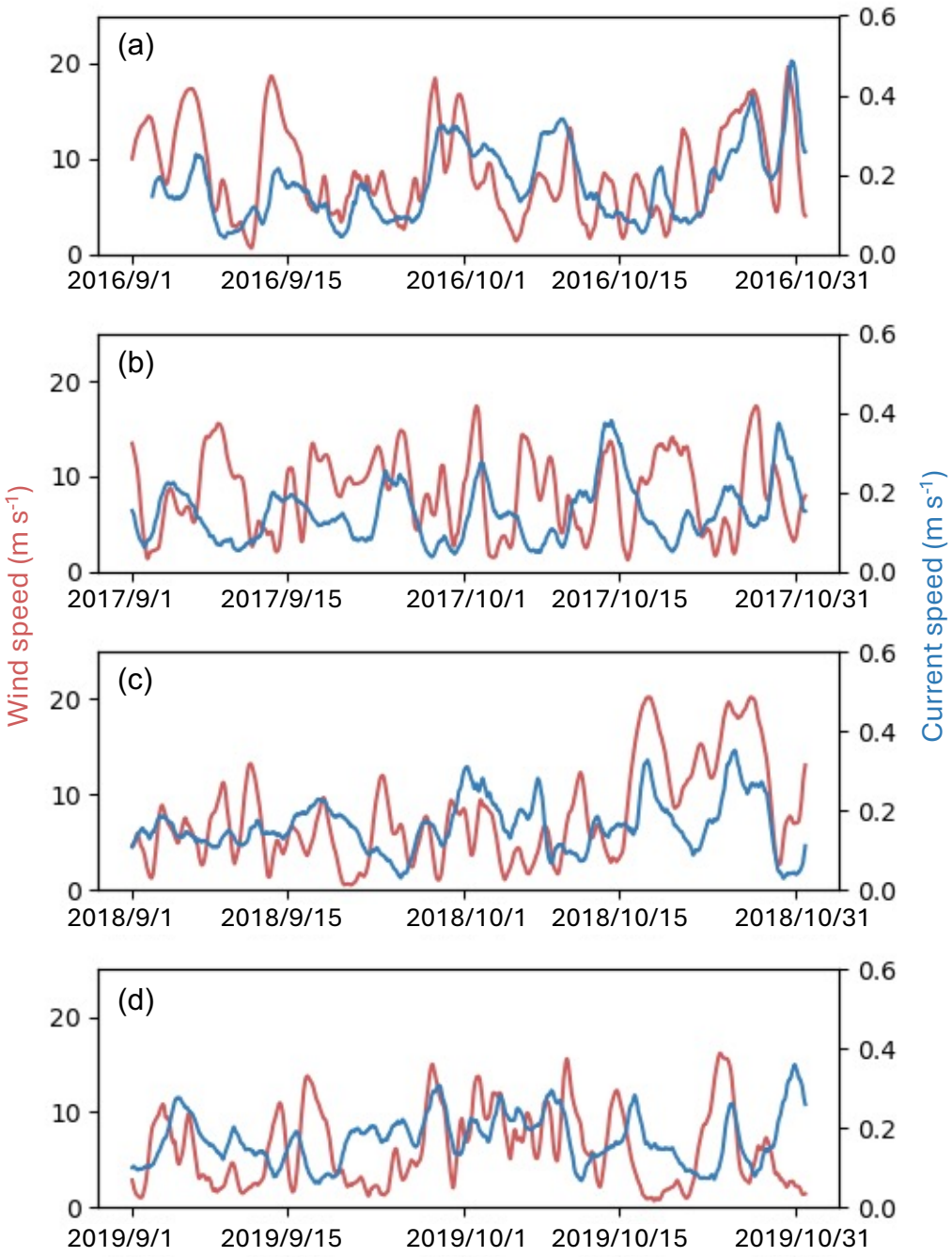

Fig. S7. Time series of the wind speed (moving average value for 20 hours) and the current speed near the bottom (moving average value for 24 hours) from September to October in (a) 2016, (b) 2017, (c) 2018, and (d) 2019.

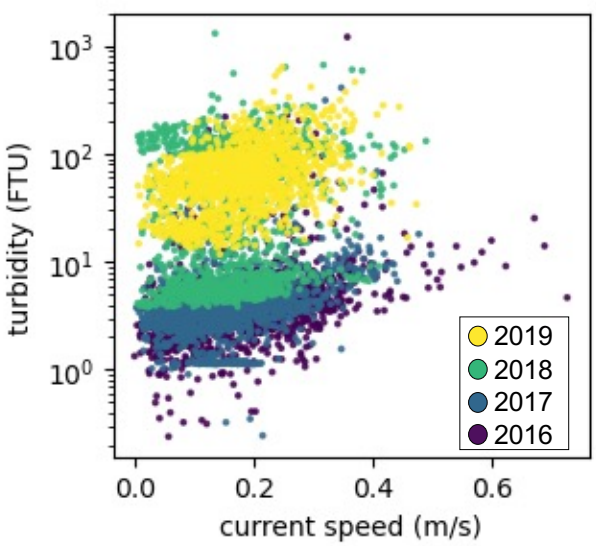

Fig. S8. Relationship between instantaneous data of current speed and turbidity near the bottom. Different colors indicate the year data was acquired.

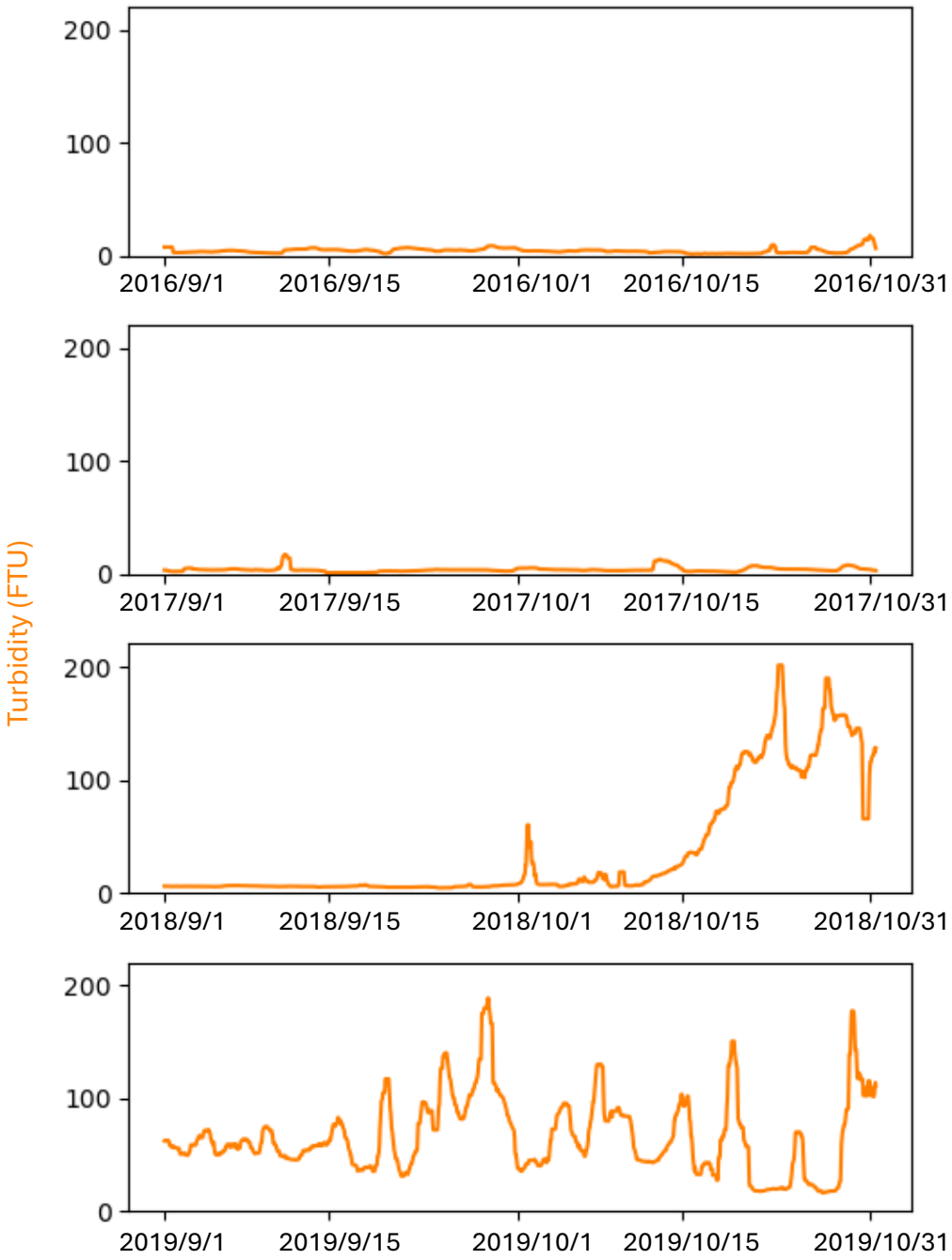

Fig. S9. Time series of the turbidity (moving median value for 24 hours) near the bottom from September to October in (a) 2016, (b) 2017, (c) 2018, and (d) 2019.

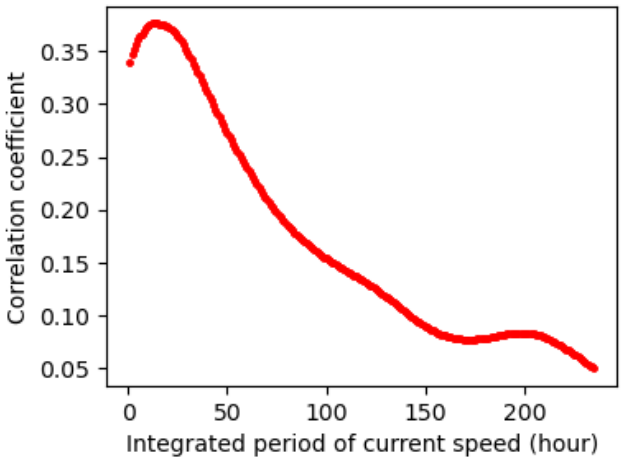

Fig. S10. The relationships between the integrated period (hour) of current speed and the correlation coefficient of the integrated current speed and the turbidity (moving median value for 24 hours).

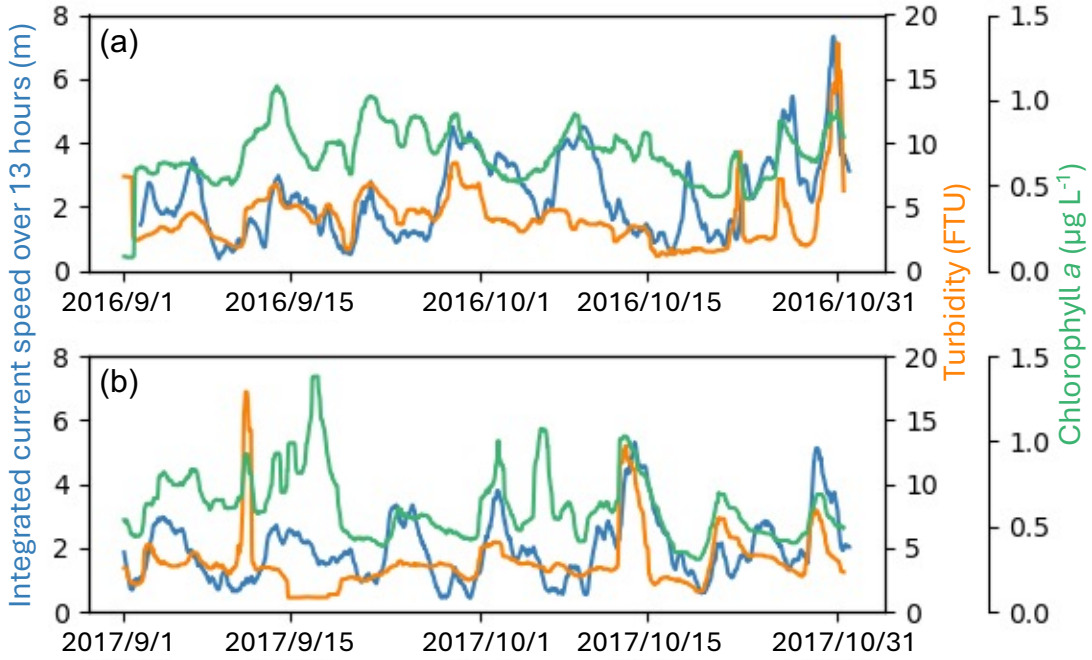

Fig. S11. Time series of the cumulative current speed over 13 hours, the turbidity (moving median value for 24 hours), the chlorophyll *a* concentration (moving median value for 24 hours) near the bottom from September to October in (a) 2016, (b) 2017.